Mem. S.A.It. Vol. 95, 22

Memorie della

Polarization Properties of Neutron Star Low-Mass X-ray Binaries with IXPE

A. Gnarini[1]⋆, F. Capitanio[2], M. Cocchi[3], S. Fabiani[2], R. Farinelli[4], and F. Ursini[1]

[1] Università degli Studi Roma Tre, I-00146 Roma, Italy
[2] INAF Istituto di Astrofisica e Planetologia Spaziali, I-00113 Roma, Italy
[3] INAF Osservatorio Astronomico di Cagliari, I-09047, Cagliari Italy
[4] INAF OAS Bologna, I-40129 Bologna, Italy

Received: 30 November 2023; Accepted: 26 January 2024

Abstract. Accreting, Weakly magnetized Neutron Stars in Low-mass X-ray binaries (NS-LMXBs) are a fundamental laboratory to study radiation processes in the strong gravity regime. The X-ray emission of NS-LMXBs is well described by a soft thermal emission plus a harder component related to Compton scatterings in the hot electron plasma around the NS. The Imaging X-ray Polarimetry Explorer (*IXPE*) can provide for the first time X-ray polarimetric information, vital for understanding the geometry of the Comptonizing region, left unconstrained by spectroscopy alone. During the first two-year observational campaign, *IXPE* observed several bright NS-LMXBs, including both Atolls and *Z*-sources. We summarize here the main results obtained from the spectro-polarimetric analysis of *IXPE* observations, providing an in-depth interpretation of these results, including also physically motivated numerical simulations to enhance our understanding of the accreting system.

Key words. accretion, accretion disks – stars: neutron – X-rays: binaries – polarization

1. Introduction

Weakly magnetized Neutron Stars in Low-mass X-ray binaries (NS-LMXBs) accrete matter via Roche-lobe overflow from a companion star, with a mass typically lower than $\sim 1\,M_{\odot}$ or an evolved white dwarf. The presence of the NS surface stops the accretion flow forming a boundary/spreading layer between the disk and the NS surface (Inogamov & Sunyaev 1999; Suleimanov & Poutanen 2006). They are highly variable objects on timescales from months down to fraction of seconds. NS-LMXBs are traditionally classified in a few broad categories according to their joint timing and spectral properties in the classic X-ray band (1–10 keV) and following their tracks in the Hard-color/Soft-color diagrams (CCDs) or hardness-intensity diagrams (HIDs, Hasinger & van der Klis 1989; van der Klis 1989):

- Soft State *Z*-sources ($> 10^{38}$ erg/s)
- Bright Atoll sources ($10^{37} - 10^{38}$ erg/s)
- Hard State Atoll sources ($\sim 10^{36}$ erg/s)

Z-sources trace out a *Z*-shaped tracks in the CCDs and HIDs on timescales of hours to a day (see Fig. 1), consisting of three branches

⋆ E-mail: andrea.gnarini@uniroma3.it

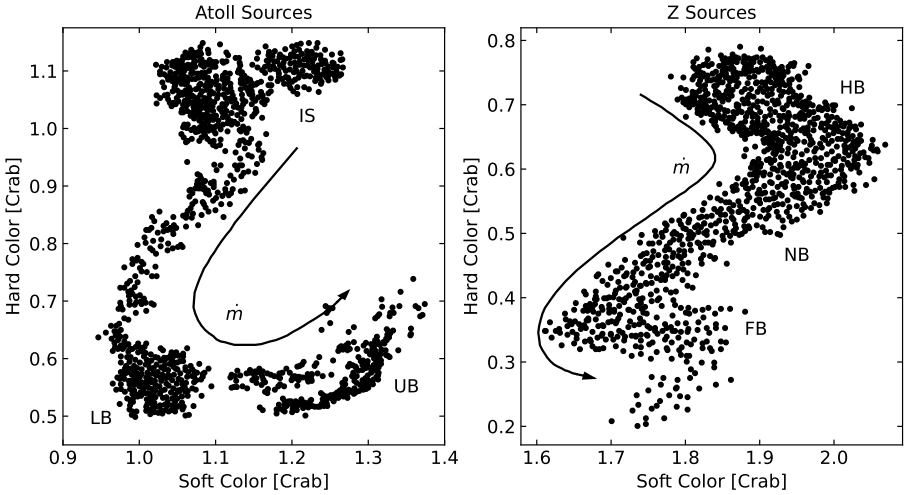

Fig. 1. Typical CCD diagrams for Atoll- and *Z*-sources, with the expected direction of increasing mass accretion rate $\dot{m}$. Atoll-sources are found in the *island state* (IS) or in the *banana state*, moving between the *lower* (LB) and *upper banana* (UB) branches. *Z*-sources moves along the three branches of the *Z*-track: the *horizontal* (HB), the *normal* (NB) and the *flaring* branch (FB). Adapted from Migliari & Fender 2006.

(Hasinger & van der Klis 1989): the *Horizontal Branch* (HB), the *Normal Branch* (NB) and the *Flaring Branch* (FB). The luminosities and the accretion rate increase as the sources move from the HB to the FB (Migliari & Fender 2006). Atoll-sources cover a wide range in luminosities, from 0.1% $L_{\rm Edd}$ up to about 50% $L_{\rm Edd}$ (van der Klis 2006), accreting at relatively low rates (compared to *Z*-sources). Many of these sources frequently exhibit X-ray bursts. At high luminosities, atoll-sources trace out a well-defined curved *banana branch* in the CCDs or HIDs (see Fig. 1), along which sources move on timescales of hours to day. The harder regions of the CCD patterns are traced out at lower luminosities and the motion is often much slower, forming isolated patches in the CCD or HIDs (the *island state*, Hasinger & van der Klis 1989).

The X-ray emission of NS-LMXBs is generally modelled with two main spectral components: a soft thermal emission produced by the relatively cold and optically thick accretion disc and a harder component related to the inverse Compton scattering of these soft photons by the hot electron plasma in the corona or in the spreading layer close to the NS (*eastern model,* Mitsuda et al. 1984, 1989). The opposite occurs in the *western model* (White et al. 1988): the hotter NS population is directly detected and modelled by pure black-body while the cold, disc photons are Compton-upscattered by the electron corona. However, it is reasonable to think that both soft seed photon populations are scattered in the corona (Cocchi et al. 2011). Moreover, the frequent observation of a Fe emission line at $\sim$ 6 keV, especially in *Z*-sources, strongly suggests that Compton reflection by a colder medium (such as the outer accretion disc itself) is a further spectral component that needs to be taken into account (D'Aì et al. 2009; Ludlam et al. 2019; Iaria et al. 2020; Ludlam et al. 2022). While X-ray spectroscopy provides information on the physical parameters of the emitting regions (although the two emission models are largely degenerate), X-ray polarimetry is able to constrain geometrical properties, such as the shape and the extension of the Comptonizing region. In fact, different geometries result in different values and behaviour of the polarization degree (PD) and polarization angle (PA; Gnarini et al. 2022).

2. IXPE

The *Imaging X-ray Polarimetry Explorer* (*IXPE*; Weisskopf et al. 2022) is a NASA/ASI mission successfully launched on 2021 December 9 providing for the first time space, energy and time resolved polarimetry. *IXPE* operates in the 2–8 keV band and is equipped with three identical X-ray telescopes with polarization-sensitive imaging detectors (the *gas-pixel detectors*; Costa et al. 2001). With respect to previous X-ray polarimetric missions, *IXPE* provides imaging capability with $\leq$ 30 arcsec angular resolution over $>$ 11 arcmin field of view, together with 1–2 μs timing accuracy and moderate spectral resolution.

3. Results

During the first two-year campaign, several NS-LMXBs were observed by *IXPE*, including both Atoll (i.e. GS 1826–238, GX 9+9 and 4U 1820–303) and *Z*-sources (Cyg X–2, XTE J1701–462 and GX 5–1). The observational results can be compared with theoretical expectations. In particular, the X-ray polarized radiation coming from weakly magnetized NS-LMXBs can be computed with the general relativistic radiative transfer Monte Carlo code MONK, suitably adapted for NS-LMXBs (Zhang et al. 2019; Gnarini et al. 2022). As expected, the polarization degree and angle strongly depend on the geometries of the Comptonizing region and the viewing angles of the source (Gnarini et al. 2022; Capitanio et al. 2023; Ursini et al. 2023). More symmetric configurations result in lower polarization. In addition, the higher the inclination of the system, the higher the polarized signal.

3.1. Atoll-sources

In Atoll sources, the observed polarization results to be generally rather weak (less than $1.5 - 2\%$ in the whole *IXPE* band; Table 1) but with a strong energy dependence. The first Atoll observed was GS 1826–238 and only a 3σ upper limit of 1.3% was obtained (Capitanio et al. 2023). No reflection features were detected. This low polarized signal seems to rule out a radially extended X-ray emitting region seen at high inclination as the main source of the polarization, while it is more consistent with a (quasi)-spherical configuration of the Comptonizing region (Gnarini et al. 2022).

The second observed Atoll GX 9+9 shows a polarization of $\sim$ 2%, with an indication of an increasing trend with energy (Ursini et al. 2023). In this source, a reflection component is detected and the observed polarization can be explained by the combination of Comptonization in a boundary layer plus reflection. Indeed, a spreading layer-like geometry is not able to produce the entire polarized single for the inferred inclination of the source, and highly polarized reflected photons contribute to the polarization even if their fraction to the total flux is small ($\sim$ 6%). The observed spectrum of GX 9+9 is very similar to that of GS 1826–238, with similar fluxes and spectral parameters. However, GS 1826–238 does not show any reflection features. Therefore, reflection could be precisely the difference that causes the detection of the polarized signal in GX 9+9.

In the case of the ultra-compact NS-LMXBs 4U 1820–303, the observed polarization degree strongly increases from an upper limit of $<$ 1% at lower energies to $\sim$ 10% in the 7–8 keV energy range (Di Marco et al. 2023). By fitting the NICER+*NuSTAR* spectra with a model including the disc thermal emission, the Comptonized radiation and the reflection, it can be noted that the polarization degree rapidly increases as soon as the disk component drops down to a flux below 10^{-12} ergs s^{-1} cm^{-2}. This suggests that the polarization angles of each single component of the spectrum (i.e. disk, Comptonization+reflection) are orientated differently, resulting in a decrease of the total polarization degree in the spectral range where both components are present. Therefore, the high polarization degree value in the 7–8 keV energy range is related only to Comptonization and reflection. For a spreading layer-like geometry, the expected polarization degree should be $\sim 1 - 2\%$ and reflected photons can significantly increase the polariza-

tion degree as they are highly polarized (up to $\sim 20-30\%$, Matt 1993; Poutanen et al. 1996).

3.2. Z-sources

The *Z*-sources resulted to be the most polarized weakly magnetized NS-LMXBs in the whole *IXPE* band (Table 1). The observed polarization degree seems to be related to the position along the *Z*-track (Cocchi et al. 2023; Fabiani et al. 2023): on the HB, the X-ray radiation is more polarized (up to 4–5% for XTE J1701–462 and GX 5–1) and starts decreasing moving towards the NB and FB (1–2% for Cyg X–2, XTE J1701–462 and GX 5–1). The direction of the polarization found for Cyg X–2 is consistent with that of the radio jet (i.e. perpendicular to the accretion disc, Farinelli et al. 2023), also in line with recent observation of Sco X–1 with *PolarLight* (Long et al. 2022). This result excludes the possibility that most of the observed polarization comes from an optically thick photosphere of the accretion disc, as otherwise the polarization angle would be orthogonal to the disc symmetry axis (Chandrasekhar 1960). The spectro-polarimetric fit provides only upper limits to the polarization of the soft disc emission ($\lesssim 2\%$). The classical results by Chandrasekhar (1960) are valid for the initial radiation at the bottom of a scattering medium with optical depth $\tau \gg 1$. For $\tau \lesssim 2$, the polarization can be higher than the corresponding value for a semi-infinite atmosphere, with the polarization vector aligned with the surface normal (Sunyaev & Titarchuk 1985).

The observations of transient hard tails in the spectra of *Z*-sources are strictly correlated with the HB in the CCD (D'Amico et al. 2001; Di Salvo et al. 2002; Farinelli et al. 2005) and possibly produced by scattering in a jet-like outflow (Reig & Kylafis 2016). It is thus tempting to link the strong polarimetric signal found along the HB to the accelerating mechanism (still not fully understood) that produces jet emission and possibly jet-related hard tails (Reig & Kylafis 2016). However, the contribution of the hard tails to the flux in the *IXPE* band is not expected to exceed 10% (see Paizis et al. 2006) and therefore it is not very likely that this component is responsible for a strong polarized signal. The high polarization may rather originate in the spreading layer around the NS and roughly perpendicular to the disc plane or from reflection off the disc of the NS/spreading layer Comptonized photons. The higher polarization degree value of the hard component is very difficult to explain by Comptonization alone, and reflection seems to be a crucial contribution. The reflection spectrum is produced by photons scattered by the accretion disc and these photons are highly polarized, contributing significantly to the polarization even if their fraction to the total flux is small (Matt 1993; Poutanen et al. 1996).

Table 1. PDs calculated with IXPEOBSSIM (Baldini et al. 2022) of the NS-LMXBs observed by *IXPE*.

Source	PD(2–8 keV)
GS 1826–238	$< 1.3\%$
GX 9+9	$1.4\% \pm 0.3\%$
4U 1820–303	$< 1.5\%$
Cyg X–2 (NB)	$1.8\% \pm 0.3\%$
XTE J1701–462 (HB)	$4.6\% \pm 0.4\%$
XTE J1701–462 (NB/FB)	$< 1.5\%$
GX 5–1 (HB)	$4.3\% \pm 0.3\%$
GX 5–1 (NB/FB)	$2.0\% \pm 0.3\%$

4. Conclusions

X-ray polarimetry can assess the geometry of the accreting system of NS-LMXBs and the physical processes that produce the X-ray radiation. In particular, X-ray polarimetry can distinguish between different geometries of the Comptonizing region. The polarization degree and angle are very distinctive between various geometries: an extended equatorial slab that covers the entire disc produces a strong polarized signal (as expected from classical results, see Chandrasekhar 1960; Matt 1993), while more spherical symmetric configurations (such as a shell or a spreading layer geometry) are characterized by lower polarization.

Z-sources are significantly more polarized with respect to Atolls in the 2–8 keV bands, with a higher polarization degree when the sources are on the HB and lower moving along

the NB and FB. Atoll-sources show a strong energy dependence, with polarization degree also reaching $\sim 8-10\%$ at high energies. Both these behaviours fit very well the idea that the polarization is related to the combination of Comptonization in the boundary layer (with typical PD $\sim 1-2\%$) plus reflection of soft photons off the disc (PD $\sim 15-20\%$).

Acknowledgements. The Imaging X-ray Polarimetry Explorer (*IXPE*) is a joint US and Italian mission. This research used data products provided by the *IXPE* Team (MSFC, SSDC, INAF, and INFN) and distributed with additional software tools by the High-Energy Astrophysics Science Archive Research Center (HEASARC), at NASA GSFC. The US contribution is supported by NASA and led and managed by its MSFC, with industry partner Ball Aerospace (contract NNM15AA18C). The Italian contribution is supported by ASI through contract ASI-OHBI-2022-13-I.0, agreements ASI-INAF-2022-19-HH.0 and ASI-INFN-2017.13-H0, and its SSDC with agreements ASI-INAF-2022-14-HH.0 and ASI-INFN 2021-43-HH.0, and by INAF and INFN in Italy. The authors gratefully thank the members of the TW4 and the entire *IXPE* Collaboration for all the work on *IXPE* observations made in the first two years of the *IXPE* mission.

References

Baldini, L., Bucciantini, N., Lalla, N. D., et al. 2022, SoftwareX, 19, 101194
Capitanio, F., Fabiani, S., Gnarini, A., et al. 2023, ApJ, 943, 129
Chandrasekhar, S. 1960, Radiative transfer
Cocchi, M., Farinelli, R., & Paizis, A. 2011, A&A, 529, A155
Cocchi, M., Gnarini, A., Fabiani, S., et al. 2023, A&A, 674, L10
Costa, E., Soffitta, P., Bellazzini, R., et al. 2001, Nature Astronomy, 411, 662
D'Aì, A., Iaria, R., Di Salvo, T., Matt, G., & Robba, N. R. 2009, ApJ, 693, L1
D'Amico, F., Heindl, W. A., Rothschild, R. E., & Gruber, D. E. 2001, ApJ, 547, L147
Di Marco, A., La Monaca, F., Poutanen, J., et al. 2023, ApJ, 953, L22
Di Salvo, T., Farinelli, R., Burderi, L., et al. 2002, A&A, 386, 535
Fabiani, S., Capitanio, F., Iaria, R., et al. 2023, arXiv e-prints, arXiv:2310.06788
Farinelli, R., Fabiani, S., Poutanen, J., et al. 2023, MNRAS, 519, 3681
Farinelli, R., Frontera, F., Zdziarski, A. A., et al. 2005, A&A, 434, 25
Gnarini, A., Ursini, F., Matt, G., et al. 2022, MNRAS, 514, 2561
Hasinger, G. & van der Klis, M. 1989, A&A, 225, 79
Iaria, R., Mazzola, S. M., Di Salvo, T., et al. 2020, A&A, 635, A209
Inogamov, N. A. & Sunyaev, R. A. 1999, Astronomy Letters, 25, 269
Long, X., Feng, H., Li, H., et al. 2022, ApJ, 924, L13
Ludlam, R. M., Cackett, E. M., García, J. A., et al. 2022, ApJ, 927, 112
Ludlam, R. M., Miller, J. M., Barret, D., et al. 2019, ApJ, 873, 99
Matt, G. 1993, MNRAS, 260, 663
Migliari, S. & Fender, R. P. 2006, MNRAS, 366, 79
Mitsuda, K., Inoue, H., Koyama, K., et al. 1984, Publications of the ASJ, 36, 741
Mitsuda, K., Inoue, H., Nakamura, N., & Tanaka, Y. 1989, Publications of the ASJ, 41, 97
Paizis, A., Farinelli, R., Titarchuk, L., et al. 2006, A&A, 459, 187
Poutanen, J., Nagendra, K. N., & Svensson, R. 1996, MNRAS, 283, 892
Reig, P. & Kylafis, N. 2016, A&A, 591, A24
Suleimanov, V. & Poutanen, J. 2006, MNRAS, 369, 2036
Sunyaev, R. A. & Titarchuk, L. G. 1985, A&A, 143, 374
Ursini, F., Farinelli, R., Gnarini, A., et al. 2023, A&A, 676, A20
van der Klis, M. 1989, Annual Review of A&A, 27, 517
van der Klis, M. 2006, Rapid X-ray variability, ed. W. Lewin & M. van der Klis, Cambridge Astrophysics (Cambridge University Press), 39–112
Weisskopf, M. C., Soffitta, P., Baldini, L., et al. 2022, Journal of Astronomical Telescopes, Instruments, and Systems, 8, 1
White, N. E., Stella, L., & Parmar, A. N. 1988, ApJ, 324, 363
Zhang, W., Dovčiak, M., & Bursa, M. 2019, ApJ, 875, 148